Spectrochimica Acta Part A: Molecular and Biomolecular Spectroscopy 276 (2022) 121244

Contents lists available at ScienceDirect

Spectrochimica Acta Part A: Molecular and Biomolecular Spectroscopy

journal homepage: www.elsevier.com/locate/saa

Newly found K^+-Thioflavin T competitive binding to DNA G-quadruplexes and the development of a label-free fluorescent biosensor with extra low detection limit for K^+ determination in urine samples

Khwanrudee Chitbankluai [a,b,c], Panote Thavarungkul [a,b,c,d], Proespichaya Kanatharana [a,b,d], Morakot Kaewpet [a,b], Chittanon Buranachai [a,b,c,*]

[a] Division of Physical Science, Faculty of Science, Prince of Songkla University, Hat Yai, Songkhla, 90110, Thailand
[b] Center of Excellence for Trace Analysis and Biosensor, Prince of Songkla University, Hat Yai, Songkhla, 90110, Thailand
[c] Thailand Center of Excellence in Physics, Commission on Higher Education, 328 Si Ayutthaya Road, Bangkok, 10400, Thailand
[d] Center of Excellence for Innovation in Chemistry, Faculty of Science, Prince of Songkla University, Hat Yai, Songkhla, 90110, Thailand

HIGHLIGHTS

- A label-free K^+ biosensor with extra low limit of detection was developed.
- It is based on a new finding that K^+ destabilizes G quadruplex – Thioflavin T complex.
- The sensor can be used to detect K^+ in real urine samples without interference.

GRAPHICAL ABSTRACT

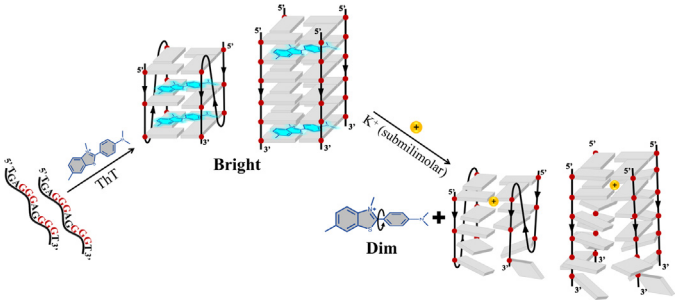

ARTICLE INFO

Article history:
Received 29 October 2021
Received in revised form 3 April 2022
Accepted 4 April 2022
Available online 8 April 2022

Keywords:
Bimolecular G-quadruplex
Tetramolecular G-quadruplex
Thioflavin T
Potassium ion
Label-free biosensor

ABSTRACT

The determination of potassium ion K^+ in body fluids is important in health monitoring and diagnoses. One of the interesting and simple methods for K^+ detection is the use of label-free biosensors based on DNA G-quadruplexes (GQs) coupled with a specific fluorescent probe, such as Thioflavin T (ThT), which lights up when bound with K^+-stabilized GQs. However, these biosensors are not generally sensitive. In this work, we found a solution: at a low concentration, K^+ competes with ThT in binding to a bimolecular GQ or a tetramolecular GQ, resulting in a decrease in ThT fluorescence emission with increasing K^+. Therefore, we developed a label-free turn-off fluorescent K^+ sensor. The sensor provides a very low detection limit of 21.87 ± 0.59 nM. Other possible interfering components in urine did not exert any effect even at quantities that were 10-fold greater than their upper limit of normal concentrations found in urine samples. With its only requirement of diluting samples, the developed low-cost label-free probe and simple sensor was successfully applied to the direct detection of K^+ in normal urine samples with high accuracy (recoveries ranged from 90% to 100%).

1. Introduction

Potassium ion K^+ plays vital roles in maintaining body functions [1,2]. It is present in blood at 3.5–5.0 mM [3], and even a slight

* Corresponding author at: Division of Physical Science, Faculty of Science, Prince of Songkla University, Hat Yai, Songkhla 90110, Thailand.
E-mail address: chittanon.b@psu.ac.th (C. Buranachai).

https://doi.org/10.1016/j.saa.2022.121244
1386-1425/

deviation from this range could cause serious complications [4]. Therefore, the determination of K^+ in body fluids is critical in diagnoses. One of the most popular methods for K^+ detection is the use of potassium ion-selective electrodes (ISEs) [5]. However, to explore the possibility of developing other simple analytical methods, several research groups have developed electrochemical [6,7] and optical K^+ biosensors [8,9]. Electrochemical K^+ biosensors are attractive because they are generally very sensitive. However, they often require complicated electrode preparation steps to ensure high selectivity and minimize interferences. By contrast, optical K^+ biosensors are less sensitive to interferences, and they can be developed to suit high-throughput applications or point-of-care detection.

One of the most popular K^+ sensing elements in optical biosensor development is the DNA G-quadruplex (GQ), which is a non-canonical tertiary DNA structure comprising layers of four guanine molecules (called G-quartets) held together by Hoogsteen hydrogen bonding [10]. In minimizing the electrostatic repulsion between guanine's carbonyl oxygens, a cation such as K^+ is inserted between two adjacent G-quartets [11]. Therefore, one can potentially quantify K^+ indirectly by measuring the amount of DNA GQs present. This measurement can be readily performed by, for example, labeling fluorescent dyes on the DNA with GQ forming sequences [12,13] or using fluorescent probes that bind specifically to DNA GQs [14,15].

A major caveat of using DNA GQs for K^+ detection is the low selectivity toward other monovalent cations, such as Na^+ [16], Pb^+ [17], and Sr^+ [18]. DNA GQs have stronger binding affinities to K^+ than to other monovalent cations [15], but their application becomes challenging when samples have a highly concentrated amount of competing cations, such as Na^+. Several research groups have attempted to solve this problem. For example, Verdian et al. [19] presented a K^+ fluorescence sensor that is based on a triple helix GQ molecular switch strategy with a detection limit of 14 μM in the presence of 2.0 mM Na^+. This sensor shows an improved selectivity but at the cost of dual labeling. For further improvement, Yang et al. developed a GQ with additional selectivity toward K^+ by using a selective amplification method [20]. In their work, they found a G-rich oligonucleotide that can form a bimolecular GQ with exceptionally high selectivity to K^+, with the selectivity coefficient being 232 (i.e., the binding to 5.0 mM K^+ is 232 times more efficient than to 150 mM Na^+). As expected, their proposed biosensor shows great selectivity toward K^+, even when used with whole blood samples. However, high selectivity often comes with a high limit of detection. In the current work, we found a solution to such problem. Our method is based on a competitive binding between K^+ and Thioflavin T (ThT) to the DNA G Quadruplexes formed from the DNA sequence used by Yang et al.

ThT, or 4-(3,6-dimethyl-1,3-benzothiazol-3-ium-2-yl)-N,N-dim ethylaniline chloride, is an interesting probe originally used for misfolded protein detection [21]. It comprises benzothiazole (BTZ) and dimethylaniline (DMA) linked by a single C–C bond. When mobile, BTZ and DMA rotate freely around a single bond [22]. If the ThT molecule is in an excited state, the rotation induces a twisted intramolecular charge transfer (TICT), which essentially quenches its fluorescence [23]. Meanwhile, the fluorescence quantum yield of ThT is significantly enhanced upon binding with large structures, such as amyloid fibrils [24], because the ThT molecule loses the rotational freedom and TICT is hindered. Numerous prior studies have reported that ThT can also emit strong fluorescence emission upon binding with DNA GQs [25,26]. ThT fluorescence is enhanced by up to 1,700 folds in the presence of DNA GQs and by only 250 folds in the presence of single-stranded DNA or double-stranded DNA [25]. Therefore, ThT is highly selective toward DNA GQs, and it has been used to probe the tendency of GQ formation in genomic DNA [25]. In addition, ThT has been widely utilized in developing GQ-based biosensors, such as those used in the detection of metal ions [27], small molecules [28], proteins [29], and DNA [30] on the basis of fluorescence measurement.

ThT–GQ-based biosensors operate on the basis of the mechanisms through which target analytes alter GQ stability. GQ stability comes from two major factors: (1) Hoogsteen base pairing among guanine that helps stabilize an individual G-quartet and (2) cations, mostly K^+, that help with screening the electrostatic repulsion between two adjacent G-quartets [11]. Therefore, agents that alter the hydrogen bonding between guanines or the presence of stabilizing cations can be potential target analytes of ThT–GQ-based biosensors. ThT is generally perceived as a reporter with a high fluorescence when GQs are stable for ThT binding, and vice versa. Interestingly, prior publications have shed new light on the issue by showing that ThT itself, at a certain extent, induces the formation of GQs even in the absence of stabilizing cations [25,31,32]. This finding helps explain why ThT is superior to similar GQ-specific dyes, such as N-methyl mesoporphyrin IX [33], in terms of binding to GQs. Nevertheless, the idea of cooperation between stabilizing cations and ThT in biosensing remains popular. For example, a novel ThT derivative, that is, ThT-E, was developed and used in conjunction with DNA GQs to detect metal ions, such as K^+ [31] and Pb^+ [17], in urine and lake water. However, the synthesis of ThT-E requires experts, and there is still room for improvement on the detection limit.

In the present study, we discovered that K^+ at low concentrations compete with ThT in the binding to a bimolecular GQ or a tetramolecular GQ formed from the DNA sequence used by the groups of Yang [20] and Sun [31]. Similar findings have been reported on thrombin competing with ThT in binding to thrombin aptamers (TBA15 and TBA29) [32,33]; the mechanism has been used to construct highly sensitive thrombin biosensors. The competition between thrombin and ThT is explained as follows: thrombin induces GQ conformation conversion from a parallel (favors ThT binding) to an antiparallel (disrupts ThT binding) one. However, to the best of our knowledge, no study has reported on K^+ being capable of converting a parallel GQ to an antiparallel one. Moreover, sensors based on competitive GQ binding between K^+ and ThT do not exist. In the current work, we show that the competition between K^+ and ThT does occur but that no evidence proves the involvement of parallel/antiparallel GQ conformational switching. In addition, competition occurs effectively only at very low concentrations of K^+. This finding leads us to develop a new GQ-based biosensor for K^+ detection. The sensor's fluorescence decreases with increasing concentration of K^+ (i.e., turn-off sensing) because of the disruptive competition between K^+ and ThT in GQ binding. Our sensor still inherits the exceptional selectivity of prior sensors [20], but it offers an unprecedented limit of detection for label-free sensing. In general, the detection of K^+ in real urine samples is challenging for optical biosensors. The proposed sensor offers a solution as it is able to perform such detection with minimal sample preparation that simply involves dilution.

2. Materials and methods

2.1. Oligonucleotides and chemicals

All oligonucleotides were synthesized and purified by high-performance liquid chromatography from Integrated DNA Technologies (IDTDNA, Singapore). The stock solutions were prepared in deionized water and stored at −20 °C in 200 μL aliquots until use. The concentration of all oligonucleotides was measured at 260 nm by ultraviolet–visible spectrophotometry using the molar

extinction coefficients from the manufacturer. The following oligonucleotide sequences were used in all experiments:

oligo-3-T 5′-TGAGGGAGGGGT-3′.
TBA15 5′-GGTTGGTGTGGTTGG-3′.
22AG 5′-AGGGTTAGGGTTAGGGTTAGGG-3′.
21CTA 5′-GGGCTAGGGCTAGGGCTAGGG-3′.
ssDNA 5′-TGCTACAGATCA-3′.

ThT, TEMED (N,N,N′,N′-Tetramethylethylenediamine) and ammonium persulfate were from Sigma-Aldrich (St. Louis, MO, USA). The ThT stock concentrations were prepared using the molar extinction coefficient of 36,000 M^{-1} at 412 nm [34]. Potassium chloride was obtained from Ajax Finechem (New South Wales, Australia). 40% acrylamide/bis-acrylamide, 19:1 solution and 10 mg/mL ethidium bromide solution were from Bio-Rad (Hercules, CA, USA). The ssDNA ladder was from Integrated DNA Technologies (10/60 Ladder, IDTDNA, Singapore) and the gel loading dye mixture (6×) was from New England Biolab (Ipswich, MA, USA). All chemicals utilized in this study were of analytical grade and used without further purification. Deionized water (18.2 MΩ cm resistivity) from a Milli-Q Direct water purification system (Millipore Corp., Billerica, MA, USA) was used throughout all the experiments.

2.2. Gel electrophoresis

Two rounds of gel electrophoresis were performed to support our hypothesis that ThT induces the formation DNA G quadruplex structures even in the absence of K^+. Both gels are 20% polyacrylamide, but the first gel along with the 1× TAE running buffer contained 6.25 μM ThT without KCl while the second gel and the 1× TAE running buffer contained 50 mM KCl without ThT. Beside the ssDNA ladder, the first lane in each gel contained oligo-3-T and the second lane contained 22AG for comparison. The DNA samples (either oligo-3-T or 22AG) were incubated in 50 mM acetate buffer solution pH 4.5 containing either ThT (for running in the first gel containing ThT) or KCl (for running in the second gel containing KCl) for 1 h at room temperature prior to mixing with the loading dye. The loading solutions contained 5.00 μM DNA and 6.25 μM ThT for the first gel or 50 mM KCl for the second gel. In each well, 10.0 μL of a loading solution was carefully filled and the gel electrophoresis was performed at 4 °C in a modified refrigerator at 100 V for 2.5 h for the gel containing ThT and 50 V for 3.5 h for the gel containing K^+. The lower voltage was used in the latter case to avoid excessive gel heating. Then the gels were stained in 0.5 μg/mL ethidium bromide dissolved in DI water for 15 min followed by rinsing in DI water for another 15 min. The gels were then imaged in a gel imaging system (Platinum HD2D-59LS-26MX, UVITEC, UK).

2.3. Circular dichroism measurement

The structural transformations of the ThT–GQ complex resulting from the addition of K^+ were investigated through the circular dichroism (CD) spectra measurement with a Jasco J-815 CD spectropolarimeter (Jasco Corp., Tokyo, Japan). The spectra were collected in the range of 200–400 nm at 25 °C with a scanning speed of 100 nm/min and a response time of 0.50 s. All CD measurements were performed in a quartz cuvette with a 1.0 mm path length. Typically, 5.0 μM of oligo-3-T was incubated with 1.0 μM ThT in a 100 mM acetate buffer solution with a pH of 5.0 and different concentrations of K^+ for 4.0 h before measurement. The background signal of the buffer solution was subtracted from all CD spectra.

2.4. Fluorescence measurement

DNA oligos and ThT were mixed in a 100 mM acetate buffer solution with a pH of 5.0 before the addition of KCl. The mixture was incubated for 4.0 h at 25 °C before being transferred to a micro quartz fluorescence cuvette with a 10 mm path length. The fluorescence measurements were performed on a fluorescence spectrophotometer (LS55, Perkin Elmer, Waltham, MA, USA). Florescence emission spectra were recorded from 470 nm to 700 nm with an excitation wavelength of 445 mm. The excitation and emission slits were set at 5 and 20 nm, respectively. The ratio of total fluorescence intensities (F_0/F) was used as the sensor response, with F_0 and F being the areas under the emission spectra in the absence and presence of K^+.

2.5. Real urine samples

Urine samples obtained from Songklanagarind Hospital (Hat Yai, Songkhla, Thailand) were used in this study. All samples were collected in polystyrene tubes and kept at −20 °C until use. Before measurement, the samples were thawed and diluted by 200,000 folds with a sodium acetate buffer solution at the optimal concentration and pH values (50 mM, pH 4.5) before use. In testing the matrix effect, a standard calibration graph and a matrix-matched calibration graph obtained from a real sample spiked with K^+ standards were plotted, and the slopes of the two graphs were compared by two-way ANOVA. If the *P* value of two slopes was greater than 0.05, the matrix effect could be ignored [35], and the concentration of K^+ in each urine sample was calculated directly from a standard calibration graph. In the case in which the matrix in real samples affected the sensor response (*P* value < 0.05), the standard addition method was used. The K^+ concentrations measured with our sensor were compared with those measured with the ISE method used in Songklanagarind Hospital to ensure accuracy.

3. Results and discussion

3.1. K^+-dependent ThT–GQ binding

The proposed binding mechanism of ThT on the bimolecular GQ or the tetramolecular GQ formed by oligo-3-T is illustrated in Fig. 1A on the basis of the measured ThT fluorescence intensities and the gel electrophoresis. As shown in Fig. 1B, the fluorescence intensity of ThT (1.0 μM) in the acetate buffer solution was weak. After the addition of oligo-3-T, the ThT peak fluorescence emission (at 495 nm) increased by ∼20 folds, thereby indicating that ThT induced two oligo-3-T sequences (5′-TGAGGGAGGGGT-3′) to form a bimolecular parallel GQ or four oligo-3-T sequences to form a tetramolecular parallel GQ structure even in the absence of K^+. This increment was unlikely to be from ThT binding on oligo-3-T in single-stranded conformation because ThT fluorescence was enhanced only by ∼1.1 folds when it bound with a single-stranded DNA with the same length and concentration (similar to those of oligo-3-T) but was not capable of forming a GQ structure even in the presence of K^+ (Fig. S1, Supplementary information). The bright fluorescence signal of ThT indicated that the rotation around the single C–C bond in the ThT molecule was restricted after the GQ binding [36]. We hypothesize that at this stage, a ThT molecule intercalated between two G-quartets (Fig. 1A at the center), thereby following existing observations regarding the interaction between ThT and bimolecular GQ in the absence of K^+ [32,33]. After the addition of a low concentration (e.g., 1.0 μM, as shown in Fig. 1B) of K^+, ThT fluorescence slightly decreased. We hypothesize that K^+ attempted to fill the space between the two

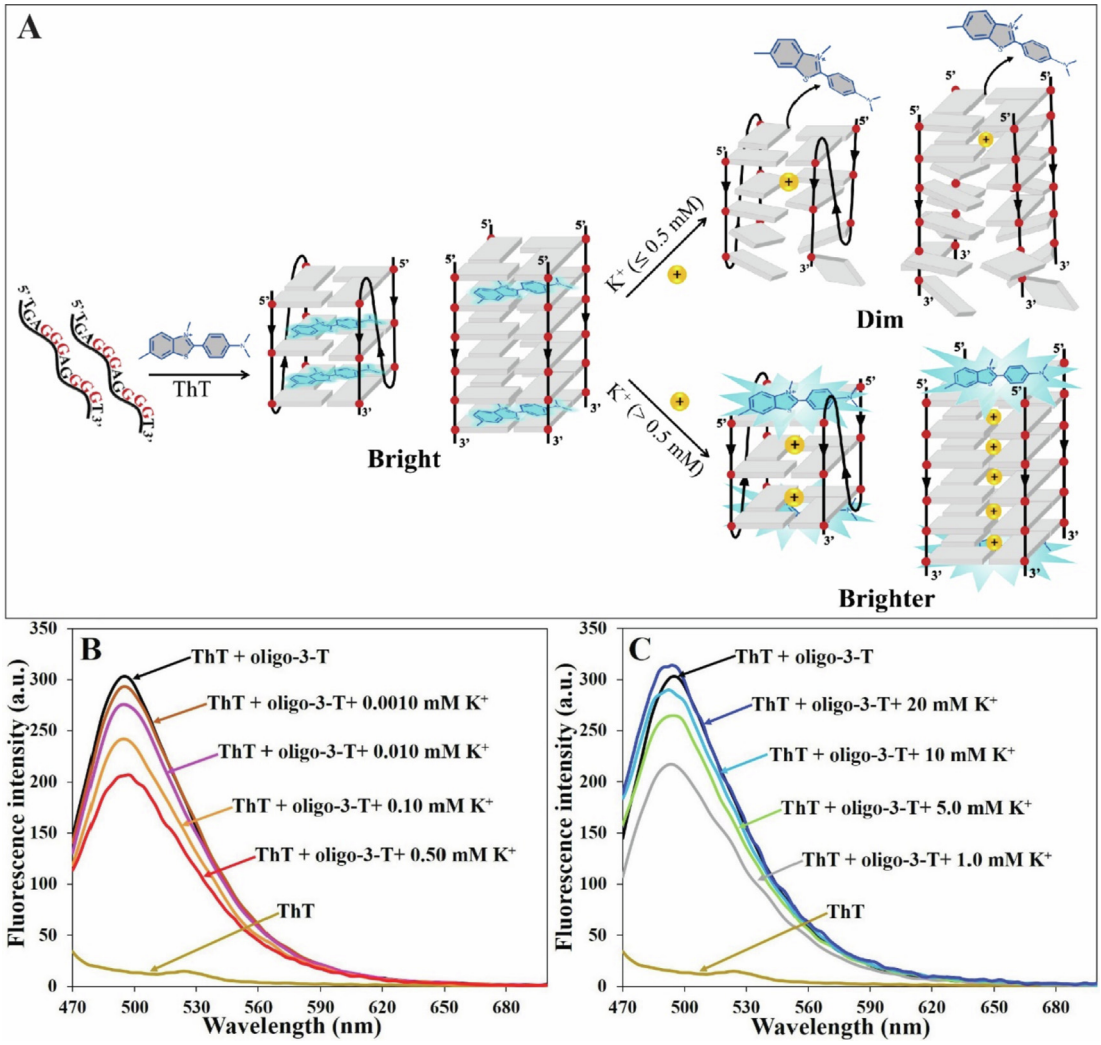

Fig. 1. **(A)** Proposed binding mechanism of ThT on the bimolecular GQ or the tetramolecular GQ formed by oligo-3-T under the influence of K^+. **(B)** Sample fluorescence emission spectra from an initial measurement showing the reduction and increase **(C)** of fluorescence intensity of ThT in the presence of oligo-3-T and different concentrations of K^+ in 100 mM acetate buffer solution (pH 5.0).

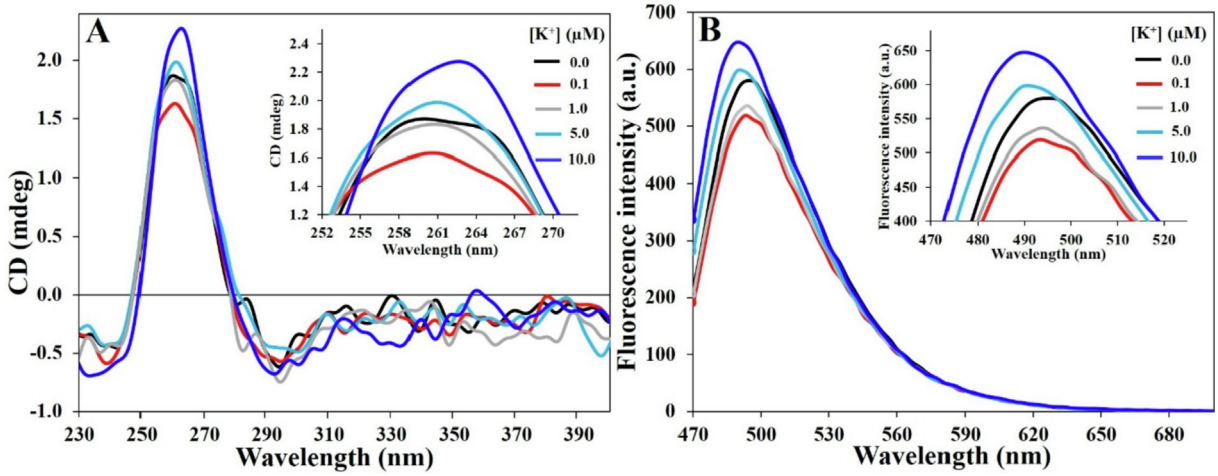

Fig. 2. **(A)** CD spectra of solutions containing 5.0 μM oligo-3-T mixed with 1.0 μM ThT and different concentrations of K^+: 0.0 μM (black line), 0.10 μM (red line), 1.0 μM (gray line), 5.0 μM (light blue line), and 10.0 μM (blue line) in the same buffer condition as that in Fig. 1. **(B)** Corresponding fluorescence spectra. Note that the concentrations of K^+ that cause the increase in ThT fluorescence are not the same as those shown in Fig. 1 because of the fact that CD spectroscopy requires high oligo-3-T concentrations to produce significant signals. Therefore, the results and discussions from CD spectroscopy may be used qualitatively. (For interpretation of the references to colour in this figure legend, the reader is referred to the web version of this article.)

G-quartets surrounded by eight carbonyl oxygens but somehow displaced the intercalating ThT molecule during the process. As the concentration of K^+ was still low, the stability of the newly formed GQ–K^+ complex was not high enough for ThT to rebind. As a result, K^+ at a low concentration caused the reduction in ThT fluorescence. Meanwhile, at high concentrations of K^+ ($\geq$1.0 mM), the ThT fluorescence increased with increasing K^+ (Fig. 1C), thus indicating an increase in ThT binding to GQ. We hypothesize that at this stage, the concentration of K^+ was high enough to stabilize the bimolecular GQ or the tetramolecular GQ structure and thus allowed ThT to stack on the top or bottom G-quartets [25], leading to an increase in ThT fluorescence.

3.2. Gel electrophoresis

From the results shown in Fig. S2 in the Supplementary information, the lanes containing oligo-3-T show 2 bands at ~20 nt and ~40 nt positions in both gels while the lanes containing 22AG show a single band. This suggests that oligo-3-T folds into a bimolecular GQ and a tetramolecular GQ in the presence of either ThT or KCl as hypothesized.

3.3. Preliminary CD spectroscopy

CD spectroscopy is used to study various secondary structures of DNA and RNA, such as duplexes in A-, B-, or Z-form; triplexes; and G-quadruplexes [37]. In addition, CD spectroscopy can differentiate GQ conformations, such as the parallel, antiparallel, or hybrid types, because of the different orientations (*anti* vs. *syn*) of the guanine bases around the sugar phosphate backbone of each strand [38]. The parallel GQ topology comprises mainly *anti* guanines, with a positive CD peak at 260–265 nm and a small negative band at 240–245 nm [38]. As for *anti* and *syn* guanines, they are often found in the antiparallel GQ topology with a positive peak at ~295 nm [39]. In this study, we used CD spectroscopy to verify the binding mechanism between ThT and GQ under the influence of K^+ (Fig. 1). As the G-rich portion of the oligo-3-T used in this study is identical to that of the oligo-3 used by Yang et al. [20], one can reasonably assume that our bimolecular GQ structure adopted the same parallel bimolecular GQ conformation as that shown in their work. Likewise, for the tetramolecular GQ, if it is a parallel structure, the CD spectra will show a positive peak at around 260 nm and that any changes in the stability of the parallel GQ conformations should result in changes in peak height.

The CD spectra of 5.0 μM oligo-3-T mixed with 1.0 μM ThT in different concentrations of K^+ are shown in Fig. 2A, along with the corresponding fluorescence spectra. In the absence of K^+ (black line), the CD spectrum showed a small negative peak at ~240 nm and a big positive peak at ~260 nm; these peaks are a signature of parallel GQ [37]. This result confirmed our hypothesis that two strands of oligo-3-T assemble to form a parallel bimolecular GQ or four strands of oligo-3-T form a parallel tetramolecular GQ with the help of ThT in the absence of K^+. In the presence of 0.10 μM K^+ (red line), the CD signal at ~260 nm decreased slightly, thus signifying that K^+ at a low concentration caused an instability in the ThT-induced bimolecular GQ or ThT-induced tetramolecular GQ. We hypothesize further that the GQ instability occurred concomitantly with some liberation of ThT and the eventual reduction in ThT fluorescence (red spectrum in Fig. 2B). Meanwhile, the CD signal at ~260 nm was recovered in the presence of 1.0 μM K^+ (Fig. 2A, gray line) and continued to increase when the concentrations of K^+ increased to 5.0 μM (Fig. 2A, light blue line) and 10.0 μM (Fig. 2A, blue line). The recoveries in CD signal at ~260 nm indicated that K^+ ions at a high concentration help stabilized the bimolecular GQ or the tetramolecular GQ structure. Therefore, the CD spectra support our hypothesis that ThT binds (likely via intercalation) and stabilizes the bimolecular GQ and the tetramolecular GQ in the absence of K^+. Interestingly, previous reports indicated a similar ThT–GQ binding mechanism [32,33] in which ThT induces TBA to form a bimolecular GQ via intercalation in the absence K^+. Then, the presence of K^+ at a low concentration (e.g., 0.10 μM) perturbs the ThT-bound bimolecular GQ or the ThT-

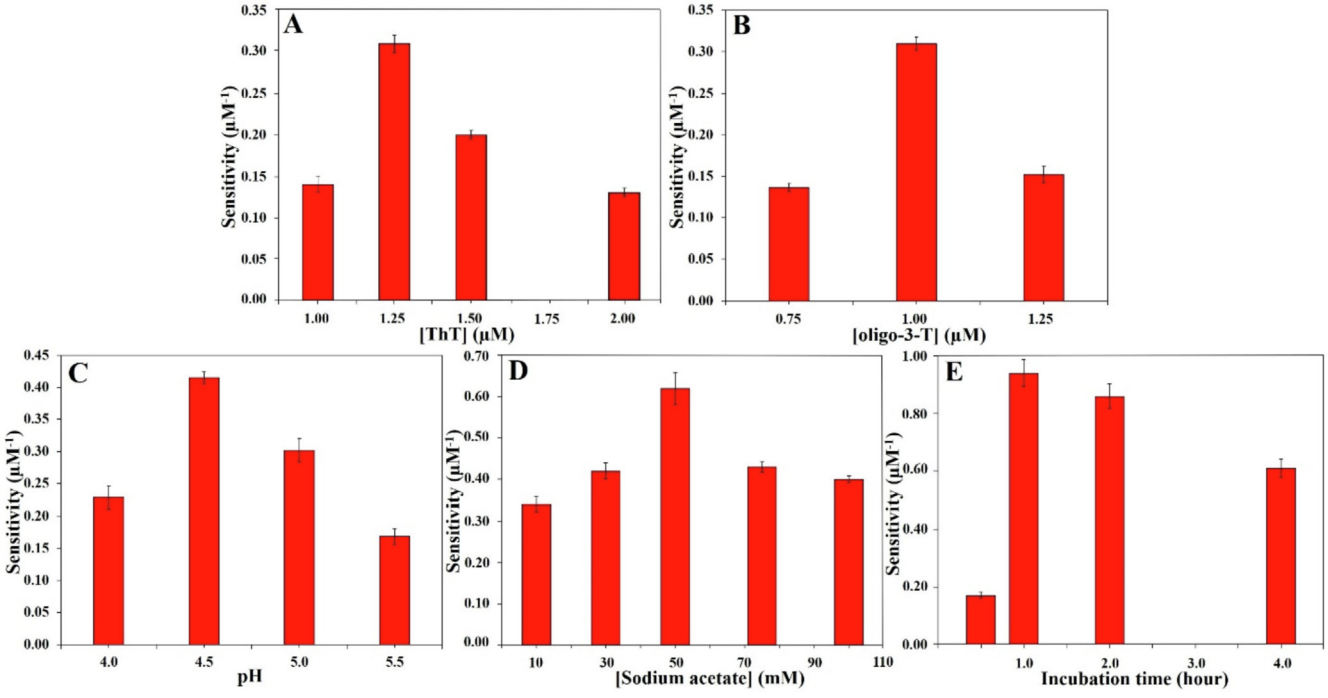

Fig. 3. Effect of various parameters on the sensitivity of sensor (slope of calibration plot): **(A)** ThT concentration, **(B)** oligo-3-T concentration, **(C)** pH of buffer solution, **(D)** buffer concentration, and **(E)** incubation time (n = 3).

bound tetramolecular GQ, whereas K^+ at a high concentration helps stabilize the complex (Fig. 1A).

3.4. Effect of K^+ on the stability of different ThT–GQ complexes

Even though ThT prefers binding to DNA GQs over single- and double-stranded DNA, it does not bind to all DNA GQ topologies equally well [40]. Therefore, we compared the disruptions of ThT–GQ complexes by diluted K^+ using four different GQs: an intermolecular parallel GQ (oligo-3-T used in this work; its G-rich portion is identical to that of oligo-3 discovered by Yang et al. [20]), an intramolecular parallel GQ (human telomeric sequence: 22AG) [25], an intramolecular antiparallel GQ (human telomeric sequence variant: 21CTA) [41], and one that can be in either intermolecular parallel or intramolecular antiparallel conformation depending on the salt conditions (thrombin aptamer: TBA15) [33]. We found that 1.25 μM ThT binds to all DNA GQs (1.0 μM) in the absence of K^+, as observed from the high ThT fluorescence signal. When the concentration of K^+ was raised from 0.0 μM to 1,000 μM, the fluorescence intensity in the case of ThT–oligo-3-T and ThT–TBA decreased by 1.8 and 1.2 folds, respectively. By contrast, the fluorescence intensity in the case of ThT–22AG showed a 2.2-fold increase while that in the case of 21CTA remained virtually unchanged (Fig. S3, Supplementary information). We found these results interesting because in the absence of K^+, oligo-3-T and TBA15 are likely to form bimolecular parallel GQs [32,33]. Meanwhile, no prior study has reported that 22AG and 21CTA are capable of doing so. Therefore, the reduction in ThT fluorescence by the low concentration of K^+ could have mainly occurred with the parallel bimolecular GQ or the parallel tetramolecular GQ conformation.

3.5. Detection of K^+ in aqueous solution

As the ThT–oligo-3-T complex is highly sensitive to the presence of K^+ at a low concentration, we propose to use the complex as a biosensor to detect K^+. As no labeling is required, the biosensor is highly simple. According to the fact that it responds to a low concentration of K^+, it could handle samples with colors through a simple dilution. In ensuring an optimal performance, some important parameters including the concentrations of ThT and oligo-3-T, the pH and concentration of the buffer solution, and incubation time were optimized. Herein, the optimization was performed by varying one parameter while keeping the others fixed. The values resulting in the highest sensitivity were then selected as the optimal condition. The sensor's sensitivities were the slope of the plot between the ratio of total fluorescence intensity in the absence and presence of K^+ (F_0/F) versus the K^+ concentrations at 0.050, 0.10, 0.20, 0.30, 0.40, and 0.50 μM.

3.5.1. ThT and oligo-3-T concentrations

First, the concentration of oligo-3-T was fixed at 1.0 μM while the concentrations of ThT were varied from 1.0 μM to 2.0 μM. Fig. 3A shows that the increase of ThT concentrations from 1.00 μM to 1.25 μM resulted in an increase in sensitivity (slope of the calibration plot) possibly because of the fact that increasing ThT in this concentration range helps stabilize the bimolecular GQ and the tetramolecular GQ, thereby making the reduction in ThT fluorescence increasingly pronounce in the presence of K^+. However, the sensitivity declined when the ThT concentrations were raised to 1.50 and 2.00 μM. We hypothesize that the abundance of ThT molecules results in highly stable ThT–GQ complexes, which are more difficult for K^+ to disrupt. Therefore, 1.25 μM was chosen as the optimal concentration of ThT in this study. Second, the concentration of oligo-3-T was optimized, with 1.0 μM yielding the highest sensitivity (Fig. 3B). We believe that at a low concentration (0.75 μM), an excessively low amount of GQ was formed such that the sensitivity was reduced. At a high concentration (1.25 μM), an excess amount of oligo-3-T could bind with K^+ without ThT, resulting in low sensitivity. Thus, 1.0 μM was chosen as the optimal concentration of oligo-3-T.

3.5.2. pH of buffer

ThT binding efficiency may be affected by the pH of the buffer solution because the protonation of nitrogen atoms in ThT in an acidic solution increases the ability of ThT to induce oligo-3-T to fold into a bimolecular GQ or a tetramolecular GQ and emits intense fluorescence [42]. Therefore, the buffer pH was tested in the range of 4.0–5.5. Fig. 3C shows that the decrease of pH values from 5.5 to 4.5 resulted in increasing sensor sensitivity possibly because numerous ThT molecules were protonated as the pH dropped, resulting in efficient ThT–GQ binding and high fluorescence enhancement before the addition of K^+. However, the sensitivity dropped at pH 4.0. We hypothesize that excessive protonation could lead to extra ThT–GQ stability that hinders ThT displacement by K^+. Thus, a pH of 4.5 was selected as the optimal pH value in this work.

3.5.3. Buffer concentration

Ionic strength could affect the stability of GQ structures [43]. Hence, the concentration of the sodium acetate buffer solution in

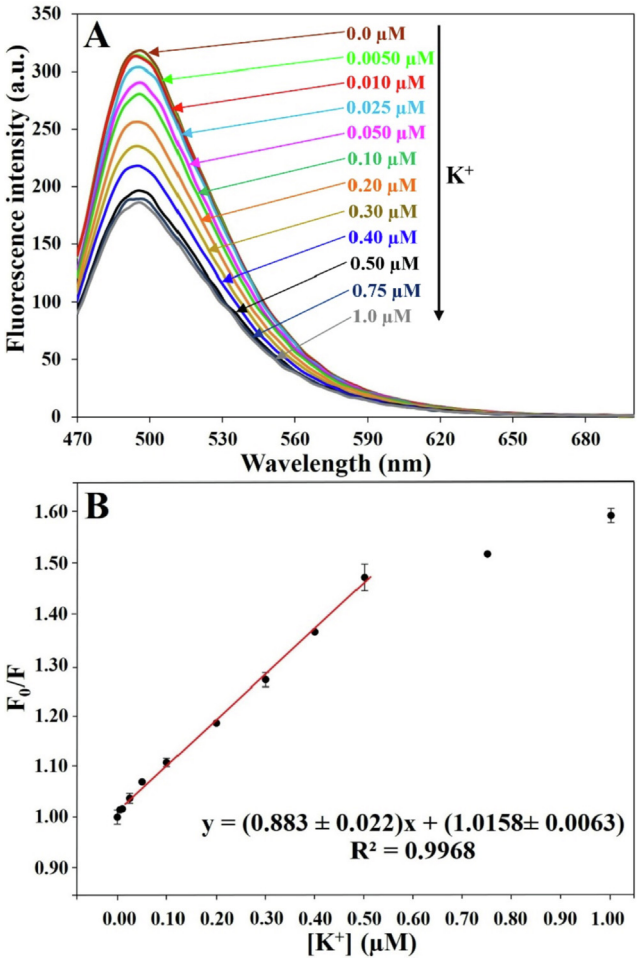

Fig. 4. (A) Fluorescence emission spectra and **(B)** plot of F_0/F ratio at different concentrations of K^+ (0.0050–1.0 μM). The linear relationship in Fig. 4B was plotted between F_0/F and K^+ concentrations ranging from 0.025 μM to 0.500 μM. The error bars indicate standard deviations (n = 3).

this work was optimized. As shown in Fig. 3D, the sensitivity of the sensor increased from 0.342 ± 0.016 μM^{-1} to 0.631 ± 0.032 μM^{-1} when the concentrations of the buffer increased from 10 mM to 50 mM. This result was likely due to the increase of Na^+ in the buffer stabilizing the GQ structures and resulting in an enhancement of the ThT fluorescence signal. However, a further increase in buffer concentration reduced the sensitivity. A possible reason is that a high Na^+ concentration could have over-stabilized the GQ structure, thereby resulting in a drop in the response toward K^+. Therefore, 50 mM was chosen as the optimal buffer concentration.

3.5.4. Incubation time

The incubation time for K^+ to displace ThT from the ThT–GQ complexes was optimized. We varied the incubation times from 0.50 h to 4.0 h. The sensitivity sharply increased when the incubation time was raised from 0.50 h to 1.0 h, but it decreased thereafter (Fig. 3E). Therefore, 1.0 h was selected as the optimal incubation time.

3.6. ThT-K^+ competitive binding verification

After the optimal conditions for fluorescence detection was obtained, we performed another set of experiments to verify the hypothesis that K^+ at low concentration did compete with ThT in GQ binding. First, to verify if ThT induces the formation of GQ in the absence of K^+, CD spectra of oligo-3-T titration by ThT under the optimal buffer condition (50 mM acetate buffer pH 4.5) were taken and we found that the CD signal at ~240 nm becomes more negative while that at ~260 nm become sharper and slightly increase with increasing concentration of ThT (Fig. S4 in the Supplementary information) strenghtening our hypothesis that ThT induces oligo-3-T to form a parallel bimolecular GQ or a parallel

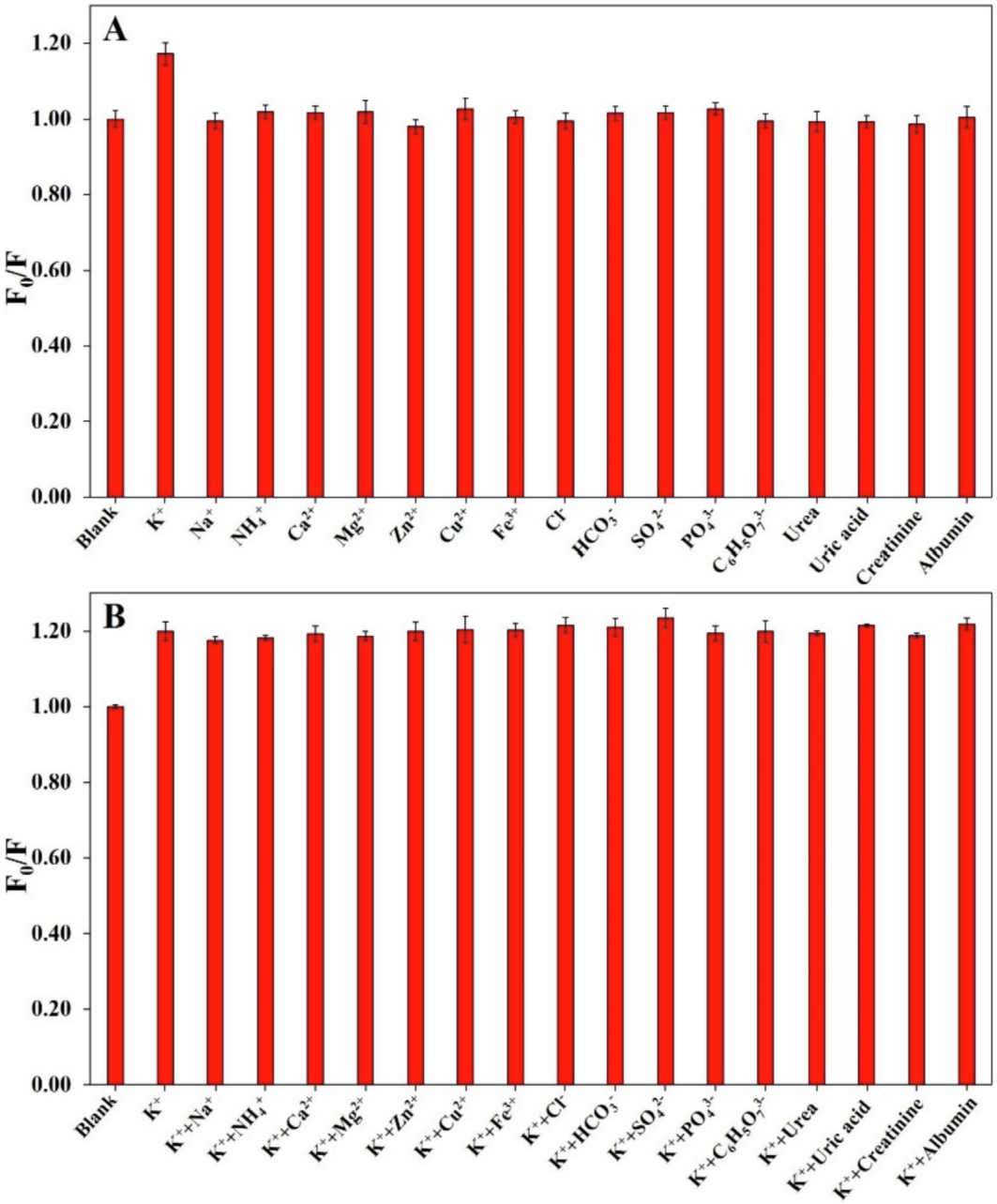

Fig. 5. Selectivity of developed sensor for K^+ detection. The figure shows the sensor responses to all interfering components when they are present individually **(A)** or mixed with 0.20 μM K^+ **(B)**. The error bars indicate standard deviations (n = 3).

tetramolecular GQ structure. Next, to confirm that K^+ at low concentrations do compete with ThT in GQ binding, we performed a dialysis experiment. First, we incubated 5.00 μM oligo-3-T and 6.25 μM ThT in 50 mM acetate buffer pH 4.5 at 25 °C for 1 h to obtain ThT-stabilized GQs. Then 500 μL of the mixture was filled inside a dialysis bag with the molecular weight cut off (MWCO) at 3,500 Da (No. 68035, SnakeSkin Dialysis Tubing, Thermo Scientific, U.S.A.). With this low MWCO, it is expected that ThT readily passes through the dialysis membrane while the DNA should be largely retained. The filled dialysis bag was then suspended in a beaker containing 5.0 ml of 50 mM acetate buffer solutions pH 4.5 with various concentrations of K^+ (0.0, 0.50, 1.0, 1.5, 2.5 and 5.0 μM). After 30 min, the absorption spectra of the solutions inside the dialysis bag were taken. It was found that the absorbance of ThT (at ~425 nm) decreased with increasing concentration of K^+, which indicated that ThT molecules were lost from dialysis bag in the presence of K^+ (Fig. S5 in the Supplementary information). Therefore, it is likely that K^+ competes with ThT and displaces the dye from GQs. The observation from the dialysis experiment was then confirmed by another set of CD spectra measurements of 5.00 μM oligo-3-T mixed with 6.25 μM ThT upon addition of K^+ in the range of 0.0 to 5.0 μM (approximately 5 times over the concentration range used in the fluorescence measurement) to retain the same stoichiometry of the reactants. It is unfortunate that the concentrations of oligo-3-T and ThT in the CD measurement cannot be as low as that used in the fluorescence measurements because the CD signal will be too low otherwise. It was found that the CD signal at ~260 nm continues to decrease while that at ~240 nm becomes less negative with increasing concentration of K^+ (Fig. S6 in the Supplementary information). This supports the hypothesis that increasing K^+ in a low concentration range destabilizes the parallel GQ structures, which likely results in the displacement of ThT.

3.7. Analytical performance

The performance of the sensor was explored by measuring the sensor response to standard K^+ solutions under optimal conditions. The fluorescence intensity of the sensor decreased with the increasing concentration of K^+ (Fig. 4A). The plot between F_0/F and K^+ concentrations showed a linear relationship in the range of 0.025–0.500 μM (Fig. 4B). The limit of detection (LOD = $3S_a/b$) was 21.87 ± 0.59 nM, and the limit of quantitation (LOQ = $10S_a/b$) was 72.9 ± 2.0 nM; here, S_a is the standard deviation of the intercept, and b is the slope of the calibration graph [44]. Interestingly, the LOD value was extremely (approximately 5,000,000 times) lower than the upper limit of urinary K^+ excretion [45] and somewhat lower than the values reported in most prior publications (Table S1, Supplementary information). This condition could make our sensor extremely suitable for detecting K^+ in complex samples, such as urine, because the matrix effects could be minimized simply by sample dilution.

3.8. Selectivity

The selectivity of the sensor was tested by comparing the sensor response (F_0/F) to K^+ at 0.20 μM (approximately at the middle of the calibration graph) and to potential interfering ionic species normally found in urine (at 10 times more concentrated than the maximum levels) [45–47], which include Na^+, Ca^+, Mg^{2+}, NH_4^+, Zn^{2+}, Cu^{2+}, Fe^{3+}, Cl^-, HCO_3^-, SO_4^{2-}, PO_4^{3-}, and $C_6H_5O_7^{3-}$. In addition, other possible interfering compounds, such as urea, uric acid, creatinine, and albumin, were tested at concentrations that are 10 times the maximum levels found in normal urine samples [45]. The other interferences found at low levels in urine, such as ascorbic acid [48], were not tested. Fig. 5A clearly shows that the sensor responses to all potential interfering species did not significantly deviate from those of the blank. As shown in Fig. 5B, the sensor responses to 0.20 μM K^+ with or without the potential interfering species were not significantly different even when they were present at concentrations that are 10 times the maximum levels found in urine. We explain that the good selectivity toward K^+ detection comes from the fact that only K^+ can cause a competitive displacement of ThT from the GQ structures. Therefore, our sensor is highly selective toward K^+ and could potentially be used with real urine samples.

3.9. Real sample analysis

To demonstrate the practicality of the developed sensor, we used it to detect K^+ in real urine samples from a local hospital. Six urine samples were collected and spiked with K^+ to the final

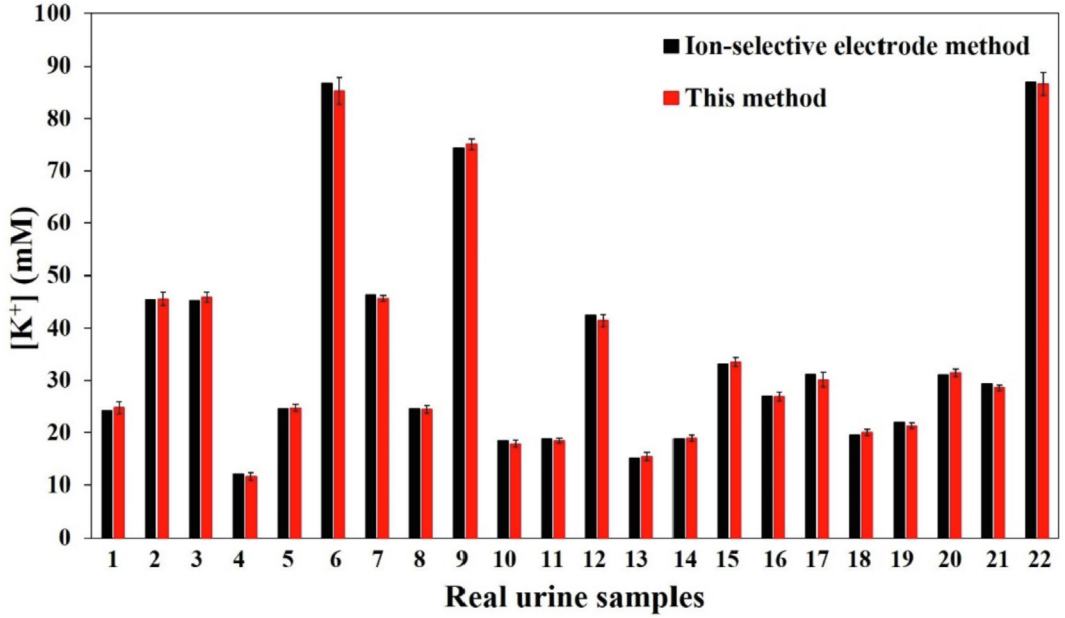

Fig. 6. Comparison of K^+ concentrations measured from our sensor and the reference values obtained from the ion-selective electrode (ISE) method used by the hospital.

concentrations of 5.0, 10.0, 20.0, and 25.0 mM before being diluted with a buffer solution and mixed with ThT and oligo-3-T. At the end, the urine samples were diluted 2×10^5 times such that the total K^+ concentrations (i.e., original plus fortified concentrations) in all the urine samples fell within the linear detection range of the sensor. This large dilution factor could be beneficial because any matrix present in the real sample will be highly diluted. Then, the sensor responses were measured under the optimal conditions. To check the effect of the matrix in the urine samples, F_0/F was plotted against the K^+ concentration to obtain a calibration graph, which was then compared with a standard calibration graph. The sensitivities of the two graphs were not significantly different (P value > 0.05). The results of the two-way ANOVA indicated that the matrix in the urine samples did not affect the sensor performance and could thus be ignored at this dilution factor. Therefore, the concentration of K^+ in real urine samples could be calculated directly from the standard calibration graph. The obtained K^+ concentrations were compared with those obtained by the ion-selective electrode (ISE) used by the hospital. The results from the two methods (Fig. 6) were not significantly different (Wilcoxon signed rank test (P value > 0.05)).

The recoveries were also calculated and found to be between 90% and 100% (Table S2), which are within the acceptable recovery range (90–107% for 100 mg L^{-1} or 2.56 mM of K^+ and 95–105% for 1000 mg L^{-1} or 25.58 mM of K^+) according to the AOAC guideline [49]. Therefore, the results from the real urine sample analysis indicated that despite being very simple, our K^+ sensor is highly sensitive and reliable and can be applied to complex biological samples.

4. Conclusion

In this work, we found that K^+, when present at a low concentration (25.0–500 nM), causes a reduction in ThT fluorescence likely because of the displacement of the dye from the ThT–bimolecular GQ or ThT-tetramolecular GQ. This finding goes against the conventional wisdom that K^+ helps stabilize the GQ structure suitable for ThT binding and results in the increase in ThT fluorescence emission. In other words, our finding suggests that depending on the concentration, K^+ can be either the competitor or supporter of ThT in GQ binding. We applied the finding to develop a label-free yet very sensitive biosensor for K^+ detection in urine samples. The developed sensor was simple yet highly sensitive and selective toward K^+, with the LOD being 21.87 ± 0.59 nM, which was lower than the normal range of K^+ in urine samples (0.75–2.61 g L^{-1} or 19–66 mM) [45]. As the sensor is very sensitive, complex samples, such as urine, can be largely diluted to avoid the matrix effect on detection.

Ethical approval

This article does not contain any studies with human participants or animals performed by any of the authors.

CRediT authorship contribution statement

Khwanrudee Chitbankluai: Conceptualization, Methodology, Investigation, Validation, Writing – original draft, Writing – review & editing. **Panote Thavarungkul:** Supervision, Writing – review & editing. **Proespichaya Kanatharana:** Supervision. **Morakot Kaewpet:** Supervision, Validation. **Chittanon Buranachai:** Supervision, Conceptualization, Methodology, Visualization, Funding acquisition, Resources, Project administration, Writing – review & editing.

Declaration of Competing Interest

The authors declare that they have no known competing financial interests or personal relationships that could have appeared to influence the work reported in this paper.

Acknowledgments

This work was financially supported by the Thailand Center of Excellence in Physics (ThEP), Prince of Songkla University and Faculty of Science, Prince of Songkla University, Thailand (grant no. ThEP-61-PHM-PSU2), the Research Assistantship, Faculty of Science, Prince of Songkla University (contract no. 1-2560-02-007) and the Graduate School Dissertation Funding for Thesis Fiscal Year 2019. The partial support from the Center of Excellence for Trace Analysis and Biosensor (TAB-CoE) and from the Division of Physical Science, Faculty of Science, Prince of Songkla University is also gratefully acknowledged. The dialysis kits and the access to the gel imaging system were kindly provided by Dr. Aekkaraj Nualla-Ong and his students from the Division of Biological Science, Faculty of Science, Prince of Songkla University. Ethidium bromide and the access to another gel imaging facility were kindly provided by Assoc. Prof. Dr. Thitika Kitpipit, Assoc. Prof. Dr. Phuvadol Thanakiatkrai and their students from the Division of Biological Science, Faculty of Science, Prince of Songkla University. The authors would also like to thank Assoc. Prof. Dr. Chongdee Buranachai and Mr. Konthee Boonmeeprakob from the Division of Physical Science and Assoc. Prof. Dr. Warakorn Limbut from the Division of Health and Applied Sciences, Faculty of Science, Prince of Songkla University for their insightful discussion and assistance with the manuscript preparation.

Appendix A. Supplementary material

Supplementary data to this article can be found online at https://doi.org/10.1016/j.saa.2022.121244.

References

[1] H.R. Pohl, J.S. Wheeler, H.E. Murray, Sodium and potassium in health and disease, in: A. Sigel, H. Sigel, R.K.O. Sigel (Eds.), Interrelations between Essential Metal Ions and Human Diseases, Springer, Netherlands, Dordrecht, 2013, pp. 29–47.
[2] J.E. Hall, M.E. Hall, Guyton and Hall textbook of medical physiology e-Book, Elsevier Health Sci. (2020).
[3] K.D. Pagana, T.J. Pagana, Mosby's Manual of Diagnostic and Laboratory Tests-E-Book, Elsevier Health Sci. (2017).
[4] U.K. Udensi, P.B. Tchounwou, potassium homeostasis, oxidative stress, and human disease, Int. J. Clin. Exp. Physiol. 4 (2017) 111–122.
[5] Y.O. Kondratyeva, E.G. Tolstopjatova, D.O. Kirsanov, K.N. Mikhelson, Chronoamperometric and coulometric analysis with ionophore-based ion-selective electrodes: a modified theory and the potassium ion assay in serum samples, Sens. Actuators B 310 (2020) 127894.
[6] M. Jarczewska, Ł. Górski, E. Malinowska, Application of DNA aptamers as sensing layers for electrochemical detection of potassium ions, Sens. Actuators B 226 (2016) 37–43.
[7] G. Wang, L. Chen, Y. Zhu, X. He, G. Xu, X. Zhang, Development of an electrochemical sensor based on the catalysis of ferrocene actuated hemin/G-quadruplex enzyme for the detection of potassium ions, Biosens. Bioelectron. 61 (2014) 410–416.
[8] P. Kassal, M. Sigurnjak, I.M. Steinberg, Paper-based ion-selective optodes for continuous sensing: Reversible potassium ion monitoring, Talanta 193 (2019) 51–55.
[9] Z. Zhang, Q. Dou, H. Gao, B. Bai, Y. Zhang, D. Hu, et al., 30 s response time of K+ ion-selective hydrogels functionalized with 18-crown-6 ether based on QCM sensor, Adv. Healthcare Mater. 7 (2018) 1700873.
[10] J.R. Williamson, M.K. Raghuraman, T.R. Cech, Monovalent cation-induced structure of telomeric DNA: the G-quartet model, Cell 59 (1989) 871–880.
[11] J.T. Davis, G-quartets 40 years later: from 5′-GMP to molecular biology and supramolecular chemistry, Angewandte Chemie - International Edition 43 (2004) 668–698.
[12] B. Kim, I.H. Jung, M. Kang, H.-K. Shim, H.Y. Woo, Cationic conjugated polyelectrolytes-triggered conformational change of molecular beacon

aptamer for highly sensitive and selective potassium ion detection, J. Am. Chem. Soc. 134 (2012) 3133–3138.
[13] Y. Zhang, J. Tian, J. Zhai, Y. Luo, L. Wang, H. Li, et al., Fluorescence-Enhanced Potassium Ions Detection Based on Inherent Quenching Ability of Deoxyguanosines and K+-Induced Conformational Transition of G-Rich ssDNA from Duplex to G-Quadruplex Structures, J. Fluoresc. 21 (2011) 1841.
[14] L. Xu, N. Sun, L. Zhou, X. Chen, J. Wang, Q. Wang, et al., A label-free fluorescence assay for potassium ions using riboflavin as a G-quadruplex ligand, Analyst 140 (2015) 3352–3355.
[15] L. Liu, Y. Shao, J. Peng, C. Huang, H. Liu, L. Zhang, Molecular Rotor-Based Fluorescent Probe for Selective Recognition of Hybrid G-Quadruplex and as a K + Sensor, Anal. Chem. 86 (2014) 1622–1631.
[16] G. Ma, Z. Yu, W. Zhou, Y. Li, L. Fan, X. Li, Investigation of Na+ and K+ Competitively Binding with a G-Quadruplex and Discovery of a Stable K+–Na +-Quadruplex, J. Phys. Chem. B 123 (2019) 5405–5411.
[17] D. Yang, L. Shi, Z. Zhao, Y. Fu, H. Sun, Q. Li, et al., A Lead (II) Ion Sensor Based on Selective Recognition of G-quadruplex for Ethyl-substitutive Thioflavin T, ChemistrySelect 4 (2019) 10787–10791.
[18] E. Largy, A. Marchand, S. Amrane, V. Gabelica, J.-L. Mergny, Quadruplex turncoats: cation-dependent folding and stability of quadruplex-DNA double switches, J. Am. Chem. Soc. 138 (2016) 2780–2792.
[19] A. Verdian-Doghaei, M.R. Housaindokht, K. Abnous, A fluorescent aptasensor for potassium ion detection-based triple-helix molecular switch, Anal. Biochem. 466 (2014) 72–75.
[20] L. Yang, Z. Qing, C. Liu, Q. Tang, J. Li, S. Yang, et al., Direct fluorescent detection of blood potassium by ion-selective formation of intermolecular G-quadruplex and ligand binding, Anal. Chem. 88 (2016) 9285–9292.
[21] H. Levine III, Thioflavine T interaction with synthetic Alzheimer's disease β-amyloid peptides: detection of amyloid aggregation in solution, Protein Sci. 2 (1993) 404–410.
[22] M.A. Haidekker, E.A. Theodorakis, Molecular rotors—fluorescent biosensors for viscosity and flow, Org. Biomol. Chem. 5 (2007) 1669–1678.
[23] V. Stsiapura, A. Maskevich, S.A. Tikhomirov, O. Buganov, Charge transfer process determines ultrafast excited state deactivation of thioflavin T in low-viscosity solvents, J. Phys. Chem. A 114 (32) (2010) 8345–8350.
[24] M. Biancalana, S. Koide, Molecular mechanism of Thioflavin-T binding to amyloid fibrils, Biochim. Biophys. Acta Proteins Proteom. 2010 (1804) 1405–1412.
[25] J. Mohanty, N. Barooah, V. Dhamodharan, S. Harikrishna, P.I. Pradeepkumar, A. C. Bhasikuttan, Thioflavin T as an efficient inducer and selective fluorescent sensor for the human Telomeric G-Quadruplex DNA, J. Am. Chem. Soc. 135 (2013) 367–376.
[26] A. Renaud de la Faverie, A. Guédin, A. Bedrat, L.A. Yatsunyk, J.-L. Mergny, Thioflavin T as a fluorescence light-up probe for G4 formation, Nucleic Acids Res, 42(2014) e65-e.
[27] J. Ge, X.-P. Li, J.-H. Jiang, R.-Q. Yu, A highly sensitive label-free sensor for Mercury ion (Hg2+) by inhibiting thioflavin T as DNA G-quadruplexes fluorescent inducer, Talanta 122 (2014) 85–90.
[28] T. Jantarat, S. Chuaychob, C. Thammakhet-Buranachai, P. Thavarungkul, P. Kanatharana, W. Srisintorn, et al., A label-free DNA-based fluorescent sensor for cisplatin detection, Sens. Actuators B 326 (2021) 128764.
[29] D. Bai, D. Ji, J. Shang, Y. Hu, J. Gao, Z. Lin, et al., A rapid biosensor for highly sensitive protein detection based on G-quadruplex-Thioflavin T complex and terminal protection of small molecule-linked DNA, Sens. Actuators B 252 (2017) 1146–1152.
[30] W. Liu, M. Lin, X. Yang, B. Wu, N. Chen, Q. Wang, et al., Investigation of newly identified G-quadruplexes and their application to DNA detection, Analyst 141 (2016) 4463–4469.
[31] X. Sun, Q. Li, J. Xiang, L. Wang, X. Zhang, L. Lan, et al., Novel fluorescent cationic benzothiazole dye that responds to G-quadruplex aptamer as a novel K+ sensor, Analyst 142 (2017) 3352–3355.
[32] Y. Li, S. Xu, X. Wu, Q. Xu, Y. Zhao, X. Lou, et al., Thioflavin T as a fluorescence light-up probe for both parallel and antiparallel G-quadruplexes of 29-mer thrombin binding aptamer, Anal. Bioanal. Chem. 408 (2016) 8025–8036.
[33] D. Zhao, X. Dong, N. Jiang, D. Zhang, C. Liu, Selective recognition of parallel and anti-parallel thrombin-binding aptamer G-quadruplexes by different fluorescent dyes, Nucleic Acids Res. 42 (2014) 11612–11621.
[34] M. Groenning, L. Olsen, M. van de Weert, J.M. Flink, S. Frokjaer, F.S. Jørgensen, Study on the binding of Thioflavin T to β-sheet-rich and non-β-sheet cavities, J. Struct. Biol. 158 (2007) 358–369.
[35] J.N. Miller, J.C. Miller, Statistics and Chemometrics for Analytical Chemistry: Pearson/Prentice Hall, 2005.
[36] Y. Dai, Y. Zhang, W. Liao, W. Wang, L. Wu, G-quadruplex specific thioflavin T-based label-free fluorescence aptasensor for rapid detection of tetracycline, Spectrochim. Acta A 238 (2020) 118406.
[37] J. Kypr, I. Kejnovská, D. Renčiuk, M. Vorlíčková, Circular dichroism and conformational polymorphism of DNA, Nucleic Acids Res. 37 (2009) 1713–1725.
[38] D.M. Gray, J.D. Wen, C.W. Gray, R. Repges, C. Repges, G. Raabe, et al., Measured and calculated CD spectra of G-quartets stacked with the same or opposite polarities, Chirality 20 (2008) 431–440.
[39] D. Patel, A.T. Phan, V. Kuryavyi, Human telomere, oncogenic promoter and 5′-UTR G-quadruplexes: diverse higher order DNA and RNA targets for cancer therapeutics, Nucleic Acids Res. 35 (2007) 7429–7455.
[40] H. Wang, P. Peng, S. Liu, T. Li, Thioflavin T behaves as an efficient fluorescent ligand for label-free ATP aptasensor, Anal. Bioanal. Chem. 408 (2016) 7927–7934.
[41] K.W. Lim, P. Alberti, A. Guédin, L. Lacroix, J.-F. Riou, N.J. Royle, et al., Sequence variant (CTAGGG)n in the human telomere favors a G-quadruplex structure containing a G·C·G·C tetrad, Nucleic Acids Res. 37 (2009) 6239–6248.
[42] E.V. Hackl, J. Darkwah, G. Smith, I. Ermolina, Effect of acidic and basic pH on Thioflavin T absorbance and fluorescence, Eur. Biophys. J. 44 (2015) 249–261.
[43] B.G. Kim, H.M. Evans, D.N. Dubins, T.V. Chalikian, Effects of salt on the stability of a G-Quadruplex from the human c-MYC promoter, Biochemistry 54 (2015) 3420–3430.
[44] L.A. Currie, Nomenclature in evaluation of analytical methods including detection and quantification capabilities, Anal. Chim. Acta 391 (1999) 105–126.
[45] D.F. Putnam, Composition and Concentrative Properties of Human Urine, Washington, National Aeronautics and Space Administration, D.C., 1971.
[46] C.A. Burtis, E.R. Ashwood, D.E. Bruns, Tietz textbook of clinical chemistry and molecular diagnostics - E-Book, Elsevier Health Sci. (2012).
[47] S. Caroli, A. Alimonti, E. Coni, F. Petrucci, O. Senofonte, N. Violante, The assessment of reference values for elements in human biological tissues and fluids: a systematic review, Crit. Rev. Anal. Chem. 24 (1994) 363–398.
[48] J. Sendroy Jr., B.F. Miller, Renal function as a factor in the urinary excretion of ascorbic acid, J. Clin. Investig. 18 (1939) 135–140.
[49] AOAC, Guidelines for standard method performance requirements, The Association of Official Analytical Chemists International (2016) 1–18.